Available on CMS information server

CMS NOTE 1998-056

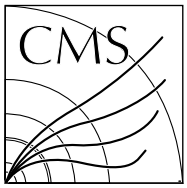

The Compact Muon Solenoid Experiment

CMS Note

Mailing address: CMS CERN, CH-1211 GENEVA 23, Switzerland

Preliminary Results from *in situ* Quartz Fiber Neutron Irradiations

N. Akchurin, S. Ayan*), E. R. McCliment, J-P. Merlo, M. Miller, Y. Önel

University of Iowa, Department of Physics, Iowa City, IA 52242 U.S.A.

W. Anderson, J. Hauptman, D. Schwellenbach

Iowa State University, Department of Physics, Ames, IA 50011 U.S.A.

Gy. Bencze

KFKI-RMKI, Budapest, Hungary

I. Dumanoğlu

Çukurova University, Department of Physics, Adana, Turkey

A. Fenyvesi, J. Molnar, D. Sohler

ATOMKI, Debrecen, Hungary

Abstract

Optical transmission characteristics of multi-mode synthetic silica-core fibers between 325 nm and 800 nm were studied *in situ* while irradiated with neutrons. In one case, fiber samples were placed near the core of a 10-kWatt reactor; in the other, fast neutrons generated by $p(18\,\mathrm{MeV}) +$ Be reaction in a cyclotron, irradiated the fibers. The neutron fluence in both studies totaled $\sim 10^{15}\,\mathrm{n/cm^2}$. Both of these initial studies indicate that in the sensitivity region of bialkiline PMTs, the irradiation induced loss is ~ 1 dB/m. These initial experiments are aimed at establishing a fiber testing methodology for assessing the expected degradation of the CMS forward calorimeter at the LHC due to large neutron backgrounds.

*) On leave from Middle East Technical University, Department of Physics, Ankara, Turkey

1 Introduction

The forward calorimeter (HF) in CMS will experience unprecedented particle fluxes. On average, 760 GeV per event is incident on the two forward calorimeters, compared to only 100 GeV for the rest of the main detector. Moreover, this energy is not uniformly distributed, but has a pronounced maximum at the highest rapidities. At $\eta = 5$ and integrated luminosity of 5×10^5 pb^{-1} (~ 10 year of LHC operation), the HF will experience ~ 1 GRad [1].

The neutron rates ($E_n \leq 14$ MeV) at the front of the detector will be of order of 10^8 Hz/cm^2. The charged hadron rates will also be extremely high, especially at the shower maximum of the HF, the rate will reach 10^{13} to 10^{16} Hz/cm^2. This hostile environment presents a unique challenge in particle detection techniques.

Since their advent, optical fibers have found diverse applications and have experienced dramatic improvements. One such emerging application is the use of silica-core and F-doped silica-clad fibers as the active component in the HF. This choice was based predominantly on their exceptional radiation resistance. In such a calorimeter, the signal is detected when charged shower particles above the Cherenkov threshold ($E > 200$ keV) generate Cherenkov light, thereby rendering the calorimeter mostly sensitive to the electromagnetic component of showers. The performance characteristics of this detector are given in detail elsewhere [2].

Although scientific literature reports the optical characteristics of these types of fibers in detail, they generally refer to the infrared band [3]: mainly three discrete wavelengths, 820, 1300 and 1550 nm. In addition, most studies are conducted with γ or electron irradiation. We concentrated on a shorter wavelength region under a neutron irradiation field, $325 \leq \lambda \leq 800$ nm, with special attention to the PMT sensitivity range, 400 to 500 nm.

2 Experimental Setup

We performed measurements at two different facilities; at a 10-kWatt experimental reactor, UTR-10, at Iowa State University (ISU) in Ames, Iowa and at the MGC-20E cyclotron of ATOMKI in Debrecen, Hungary. In the two following sections, we give brief descriptions of the facilities and the experimental setups. We paid special attention to the fact that the apparatus and the methods used to analyze data are as identical as possible.

Ocean Optics Model SD2000 spectrometer with a pulsed Xe lamp (10 Hz pulse rate) were used for all measurements. The spectral resolution was better than one nm and the data were collected within an integration time of 300 msec. A xenon lamp injects about $5-10$ μwatts of power per pulse into fibers (NA = 0.22) under test.

The types of fibers used in these initial studies are listed in Table 1. Our objective at this time was to establish a coherent methodology for testing and specifying fibers for the forward calorimeter and not to perform an exhaustive test of all available fibers.

Table 1: Types of fibers used in this study are listed below. The FSHA- and FIA-type fibers are manufactured by Polymicro Inc. (USA) and IN-type is by INFOS (Russia).

ID	Core (μm)	Clad (μm)	Buffer(μm)	OH^- (ppm)
FSHA	Silica (300)	Polymer (320)	Acrylate (345)	$\sim$700
FIA	Silica (200)	F-Silica (240)	Acrylate (500)	$<$1
IN	Silica (300)	F-Silica (316)	Polyimide (345)	$\sim$1200

2.1 ISU UTR-10 Reactor

In the core of the reactor, the optical fibers were subject to a combination of gamma-rays, fission spectrum neutrons and thermal neutrons [4]. The gamma ray dose was assumed to be fairly uniform throughout the core, while the ratio of fast-to-slow neutrons depended strongly on the location within the reactor. Figure 1 schematically shows the layout.

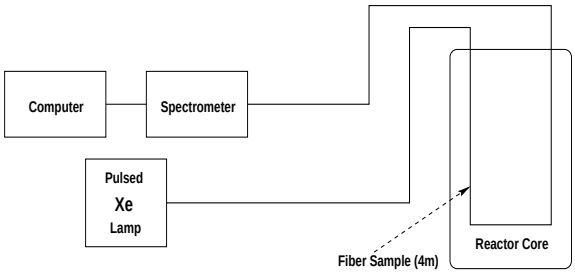

Figure 1: The sample fibers are placed close to the reactor core during the entire experiment. The light is injected from the Xe light source and transmitted through several meters of large diameter silica fibers before hitting the sample fibers; finally the transmitted light is transported once again with large diameter silica fibers and is analyzed by the spectrometer. The spectrum is stored in a personal computer for further off-line analyses.

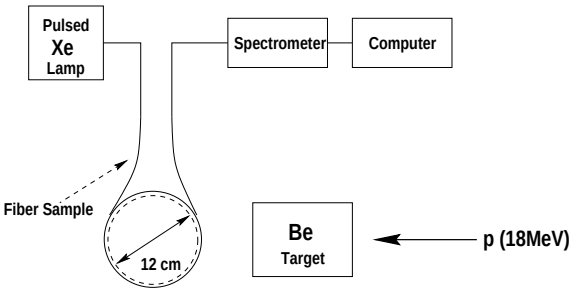

Figure 2: The sample fibers are coiled around a 12-cm diameter cylinder 5 cm away from the beryllium target. An identical set-up as in the ISU reactor collects and stores data (see Figure 1).

At the end of the experiment, the total gamma dose was estimated to be $\sim$ 22 kRad. The gamma ray dose was determined by placing commercial dosimeters in the rabbit tube (pneumatic tubes that enable placement of samples in the reactor core) which is in the reactor core. Access to the fuel region, however, was limited so that no direct dosimetry is available for this region.

The total neutron flux was determined by measuring gamma-ray activity in activated gold foils. Before the experiment, foils were activated in the fuel region and in the rabbit tube in a low-power run. The neutron-activation gamma-ray activity as a function of time was measured using Ge detectors, fitted to the known half-life and the activity at the time of irradiation was determined. The neutron flux was 1.3×10^{10} n/cm^2/s/kW and the thermal neutron flux was estimated to equal 8.5×10^9 n/cm^2/s/kW. The integrated neutron fluence at the end of the measurements was 1×10^{15} n/cm^2.

The design of the sample holders for the fibers was dictated by the geometry of the fuel elements of the reactor. The fibers were loaded into the sample holders with approximately 1/2 of the length of each fiber in 2-cm diameter loops and the remaining length straight. The entire sample holder was immersed in deionized water during reactor operations. Only the ends of the fibers were situated above the coolant water level. The temperature was not monitored near the fuel region and there may have been large temperature gradients, particularly because the sample holders were in contact with fuel elements. The reactor coolant, however, was maintained at 26.7 ^{0}C at all times via a set of automatic valves. The fibers were connected to 8 meter long transport fibers which were fed through the reactor shielding and connected to the xenon light source and spectrometer.

During the experiment, the power of the reactor was periodically altered to allow for irradiation of electronic components. This had an additional benefit of allowing us to observe often cited but not well-understood recovery phenomena, as we discuss later.

2.2 ATOMKI Cyclotron Neutron Source

18 MeV protons incident on a 3 mm thick cooled beryllium target generate neutrons with an average energy of 3.7 MeV in the forward region (see Figure 2). The energy spectrum of neutrons ranges up to 20 MeV. The target current and the collected charge were measured during irradiation and were used to derive the flux rate and the neutron flux, using data from [5]. The diameter of the proton beam was 14 mm and the target current ranged from 20 to 24 μamps. A pair of ionization chambers with different neutron and gamma response functions was used to monitor the mixed neutron-gamma field of the source and to estimate the gamma content. The total dose due to gammas was estimated to be 6.3 krad.

In the cyclotron measurements, the fibers were coiled around a 12 cm diameter cylinder and located 5

cm away from the neutron production target. The beam was perpendicular to the symmetry axis of the cylinder. The maximum neutron flux was at 0^0 and at the end of a 25.3-hour period, the total fluence was 1.02×10^{15} n/cm^2 $\pm 18\%$. The average neutron fluence at the cylinder was estimated to be 0.6×10^{15} n/cm^2. During the irradiation, the dose rate was constant at 1.1×10^{10} n/cm^2 sec $\pm 18\%$, except for a 13.26-hour down-time in order to change the ion source.

3 Analyses and Results

The usual expression for the attenuation can be written as

$$A(\lambda) = A_0(\lambda) - \frac{10}{L} \log \frac{I_{irr}(\lambda)}{I_0(\lambda)} \tag{1}$$

where $A_0(\lambda)$ is the attenuation of the fiber (dB/m) prior to irradiation, L is the length of the irradiated fiber (in our case, typically 3-4 meters) and I_{irr} and I_0 are the spectral intensities measured for irradiated and unirradiated cases, respectively. The second term represents the irradiation induced loss in the optical transmission and hereafter we refer to it as induced loss.

In all cases, the studied spectral range covered from 325 nm to 800 nm. The intensity data were binned in 25 nm intervals and the average values are used in calculations and figures.

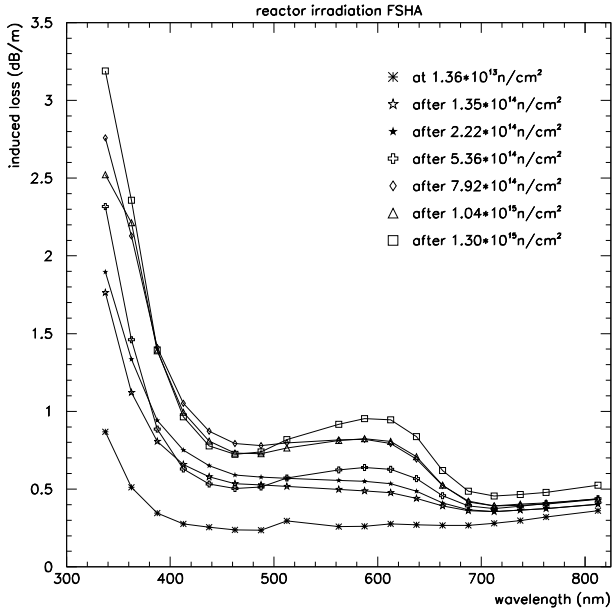

Figure 3: Neutron irradiation induced loss for the FSHA-type fiber reaches 1 dB/m after 1.3×10^{15} n/cm^2 at 600 nm at the reactor. In $400 \leq \lambda \leq 500$ nm range, the loss is on average less than 1 dB/m. Figure 5 shows by arrows at what time these seven spectra were taken (see text for details).

In near-UV and visible spectral regions, the radiation induced absorption bands in silica-core fibers can be grouped in the following manner:

1. The prominent absorbtion band in the range $\sim 600 - 630$ nm is interpreted to originate from nonbridging-oxygen hole centers (NBOHCs). The NBOHC is a molecular structure where a silicon atom is bonded to four oxygens and one of them carries an unpaired electron, $\equiv Si - O\cdot$. It was shown that a large γ-induced absorbtion band arises with F-doped silica-clad fibers compared to polymer clad fibers [6]. By progressive etch-back of F-doped silica-clad fiber and electron spin resonance (ESR), it was demonstrated that NBOHCs are located largely in the core-clad interface. The origin of these excessive NBOHCs then may be the conversion of paired hydroxyl groups near the surface of the core rod into peroxy linkages during the plasma deposition of the F-doped

cladding. The peroxy linkages would serve as NBOHC precursors by breaking of the $O-O$ bond. If this argument holds true, the production of radiation-hard fibers would mean exclusion of OH groups and peroxy linkages from the core rod. NBOHCs have a luminescence band at around 670 nm.

2. The attenuation tail that extends from near-UV to visible, the so-called UV tail, has several origins, however the strongest color center that contributes to this absorption band comes from chlorine impurities as varified by ESR studies [7].

3. E' center, one of the most studied defects in SiO_2, ($\equiv Si\cdot$), has an absorption peak at 212 nm and a luminescence at 450 nm. These color centers are produced in glasses by energetic irradiation and during the fiber drawing process [8].

4. Other absorption peaks at $\sim$ 660, 760 nm and at longer wavelengths are reported. They are of little interest for our application and we will not elaborate on them in this note.

5. It is worthwhile to note that different color centers may interact with each other and that they display different characteristics than what is listed above when irradiated [9].

3.1 Reactor Data

The spectral dependence of irradiation induced loss for the FSHA fiber displays a characteristic behavior common to most irradiated optical silica fibers in Figure 3. The near-UV region shows a rapid transmission loss with irradiation. In the 400-500 nm band, there is a soft dip and around 600 nm, there is an absorption band ascribed to NBOHCs. In the range of 700-800 nm, the attenuation increase due to irradiation seems affected the least. This feature is observed by others for high OH content fibers [10].

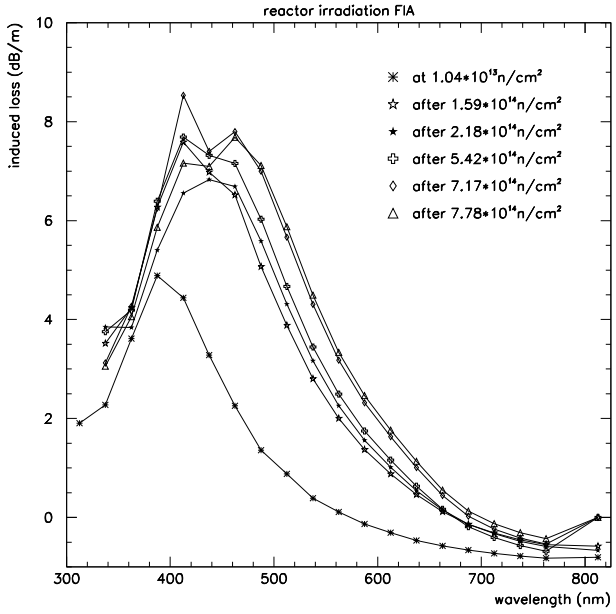

Figure 4: Neutron irradiation induced loss reaches 8 dB/m at 450 nm for the FIA-type fiber after 7.8×10^{14} n/cm^2 at the ISU reactor.

The FIA-type fiber, Figure 4, exhibits a different damage profile. The induced losses are higher, 8 dB/m at 450 nm, for similar neutron fluences compared to the FSHA-type fiber. The hydroxyls may not be readily terminating and deactivating the color centers due to reduced OH concentration (less than 1 ppm) in the core material. There is a shift in the absorption band peak from $\sim$ 390 nm at a fluence of 1.04×10^{13} n/cm^2 to 460 nm at an increased fluence of 7.78×10^{14} n/cm^2. The attenuation behavior in the region between 300 nm to 400 nm is rather uncharacteristic. It is possible that the luminescence

band at 450 nm from E′ oxygen-vacancy centers contributes to light emission and effectively reduces the attenuation here, but this region will have to be studied further.

The reactor could only be operated during the day for an 8-hour period. Figure 5 shows the history of the reactor operation in terms of the induced loss in the FSHA-type fiber. Although there are many parameters that contribute to the behavior in this figure, it is interesting to note that the attenuation reflects the neutron fluence (or more precisely the reactor power) at a given time and that the recovery occurs rather quickly when the power in the reactor is reduced or shut down (as on the second half of the first day). The increased attenuation is quickly restored, however, when the fibers are irradiated again (see the beginning of the third day, for example).

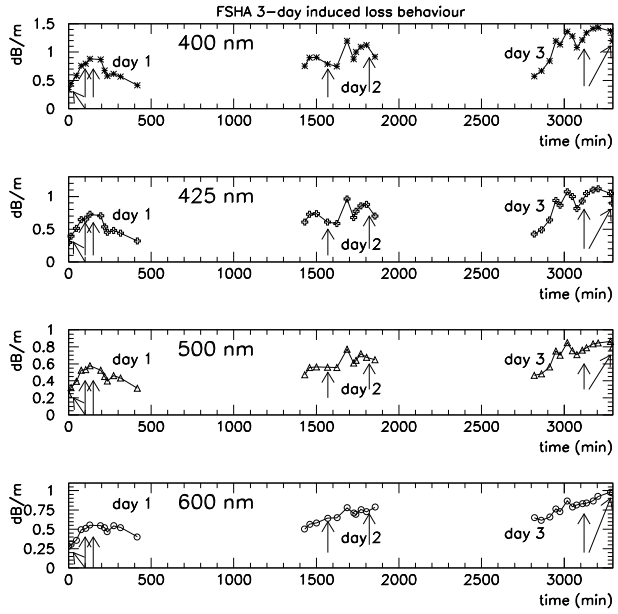

Figure 5: FSHA-type fiber induced loss curves at five different wavelengths show the power history of the reactor.

From figure 3, one can see the dynamic characteristic of the optical fiber. The first three spectra are taken in day one (see the arrows in Figure 5). The induced loss increases as the integrated neutron fluence increases for all wavelengths. The first measurement in the beginning of the second day after an over night shut-down, (indicated by open crosses) shows recovery in shorter wavelengths. The same effect is observed in the beginning of day three (going from open diamonds to open triangles).

In order to extract the kinetic behavior of attenuation with accumulated dose or neutron fluence, we fitted the data to a function of form aD^b, Figure 6. Table 2 summarizes the results. As is clearly seen from Figure 6, there are no saturation or quasi-saturation effects that would signal exhaustion of the precursors that turn into color centers. Power-law behavior suggests the activation of precursor species (and sub-species) as the dose accumulates. It is suggested in [11], however, that the silica fibers would reach their fully radiation densified state for fast neutron fluences of $\sim 10^{20}$ n/cm^2.

Within the experimental accuracy, the parameter b is the same for 400, 425 and 500 nm for both type FSHA- (high OH) and FIA-type (low OH) fibers. At 600 nm, however, presumably due to NBOHCs and the low OH content of the FIA-type fiber core, the FIA-type degrades more readily ($b \approx 0.43$) when compared to the FSHA-type fiber ($b \approx 0.26$). Similar values are reported $b = 0.295$ in [12] and $b = 0.263$ [13] for pure silica-core optical fibers.

3.2 Cyclotron Data

Figure 7 shows the induced loss for the IN-type fiber for fast neutrons. The UV-tail and the absorption band at around 630 nm are clearly observable, much like Figure 3. At 10^{15} n/cm^2, the induced loss

Table 2: Power-law behavior of irradiation induced loss with accumulated neutron fluence is shown by the fit parameters to a functional of type aD^b, where D is the neutron fluence. The parameter b is calculated at four wavelengths for FSHA, FIA and IN-type fibers. Note that the data for FSHA and FIA come from the reactor, while the IN data are from the cyclotron.

ID	400 nm	425 nm	500 nm	600 nm
FSHA	0.21	0.21	0.21	0.26
FIA	0.20	0.20	0.29	0.43
IN	0.35	0.34	0.59	0.69

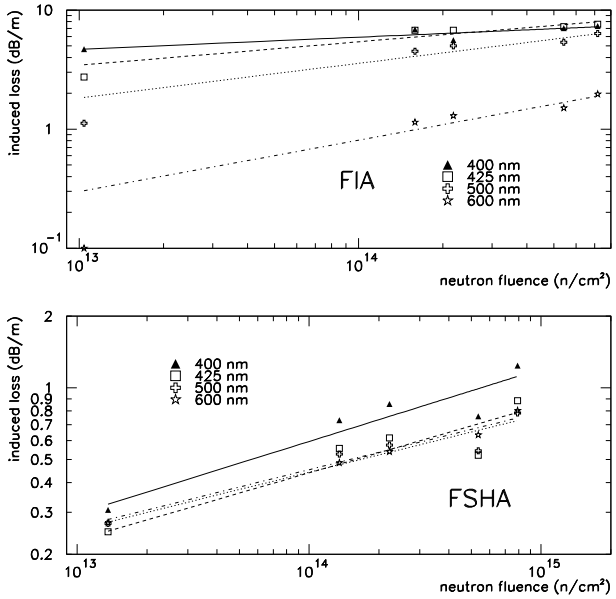

Figure 6: The power-law dependence of induced loss on neutron fluence is shown above for the FIA- and FSHA-type fibers. Within the experimental accuracy, the induced loss scales as D^b, where D is the neutron fluence. The exponent b varies between 0.20 to 0.43, depending on the wavelength (see Table 2). The solid (400 nm), dashed (425 nm), dotted (500 nm) and dash-dotted (600 nm) lines are fits to data.

in the region of interest is about 1 dB/m. Note that the neutron rate was kept constant at 1.1×10^{10} n/cm^2 sec $\pm 18\%$, except for a 13.26-hour down-time in order to change the ion source. The down-time occured towards the end of the irradiation, after the integrated neutron fluence of 7.48×10^{14} n/cm^2. Note that the next measurement (represented by open triangles), in shorter wavelengths ($\lambda \leq 500$ nm), shows less induced attenuation even though the total fluence is higher, indicating recovery during 13.26-hour shutdown. We have already described the same phenomena in the reactor experiment in the previous section.

Table 2 shows, for the IN-type fiber, the parameter b tends to be $> 50\%$ higher at the same wavelengths compared to FSHA and FIA fibers (Figure 8). There may be several reasons for this: The more energetic neutrons from the cyclotron may be more damaging compared to the mostly low-energy neutrons from a reactor, or the constant neutron dose rate may induce more optical loss or it may simply be due to a characteristic of IN-type fiber. We will investigate the rate effects in the next set of experiments.

3.3 Recovery

Essentially, all silica-core fibers tend to recover to varying degrees. In Table 3, the time constants are evaluated assuming an exponential behavior in the form of $e^{-t/\tau}$. There are undoubedly several processes that contribute to recovery phenomena. Our intent is to characterize a gross time scale for this behavior.

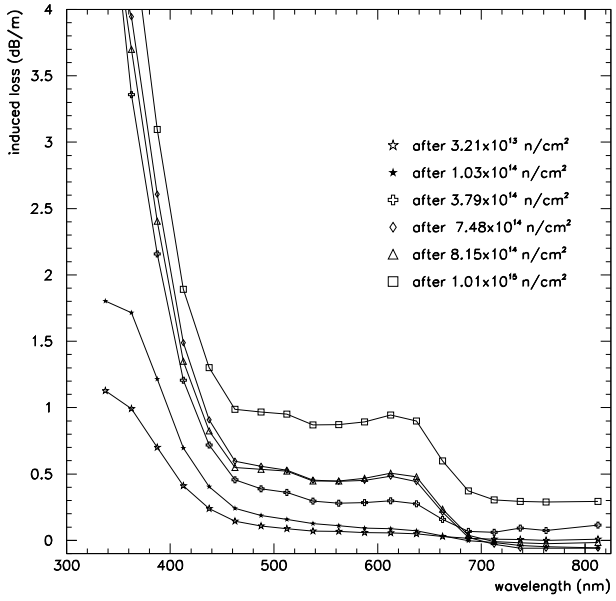

Figure 7: Neutron irradiation induced loss at 600 nm is about 1 dB/m for the IN-type fiber at the ATOMKI cyclotron. The neutron rate was kept constant at 1.1×10^{10} n/cm^2 sec $\pm 18\%$, except for a 13.26-hour down-time in order to change the ion source. After 7.48×10^{14} n/cm^2, note that the next measurement (represented by open triangles), in shorter wavelengths ($\lambda \leq 500$ nm), shows smaller induced loss, indicating recovery during 13.26-hour shutdown.

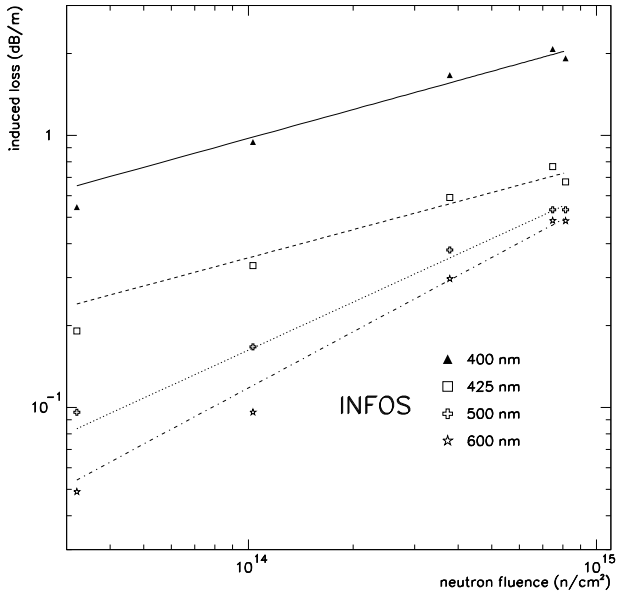

Figure 8: The power-law dependence of induced loss on neutron fluence is shown above for the IN-type fiber. The induced loss scales as D^b, where D is the neutron fluence and the exponent b is typically 0.35 to 0.69. The solid (400 nm), dashed (425 nm), dotted (500 nm) and dash-dotted (600 nm) lines are fits to data.

Similar time constants are reported in [14]; from the data presented in Figure 4 of [15], we calculate $\tau \sim 10^4$ seconds for silica-core fibers in the green wavelength region. It is also noteworthy that as Table 3 and data in [15] suggest, the recovery takes place faster in 400-500 nm band for polymer clad fibers (FSHA), compared to silica-clad fibers.

Table 3: Recovery time constants, τ (sec), are calculated at four wavelengths.

ID	400 nm	425 nm	500 nm	600 nm
FSHA	7560	6780	17100	17100
FIA	15360	9960	6540	7200
IN	9650	11760	10640	11410

Figures 9 and 10 show the recovery in the optical transmission for the FSHA- and FIA-type fibers.

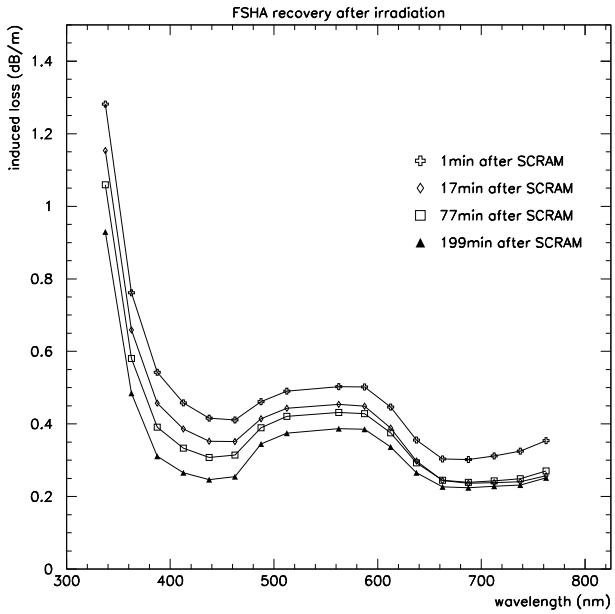

Figure 9: The post-irradiation optical transmission recovery of the FSHA-type fiber is shown above at four different times at the end of the third day of reactor operation. Note that there is a speedy recovery after 1 minute (from 1 dB/m to 0.55 dB/m at 600 nm) and that the spectral damage profile is, to a large extent, maintained during the recovery process. SCRAM refers to reactor shutdown.

4 Conclusions

1. Some recovery is observed in most silica fibers [16]. A typical time constant is evaluated to be in the order of 10^3 to 10^4 seconds. Once the radiation is reapplied to the fibers, the color centers are quickly reactivated and the optical characteristics return to the same state as at the end of irradiation. No permanent recovery is observed [10].

2. The importance of *in situ* optical measurements is manifest by the recovery data presented here. This is particulary important for calorimetry and the calibration of the forward calorimeter. The neutron rate at the cyclotron was constant at 10^{10} Hz/cm^2; and at the reactor, the rate was varied but the average rate over the coarse of three days amounted to 6×10^9 Hz/cm^2. These rates are more by one or two orders of magnitude compared to what is expected by the MARS code in the front of the HF [17]. We plan to study rate effects in more detail.

3. The luminescence properties of the fibers need to be studied in detail and their effect on the

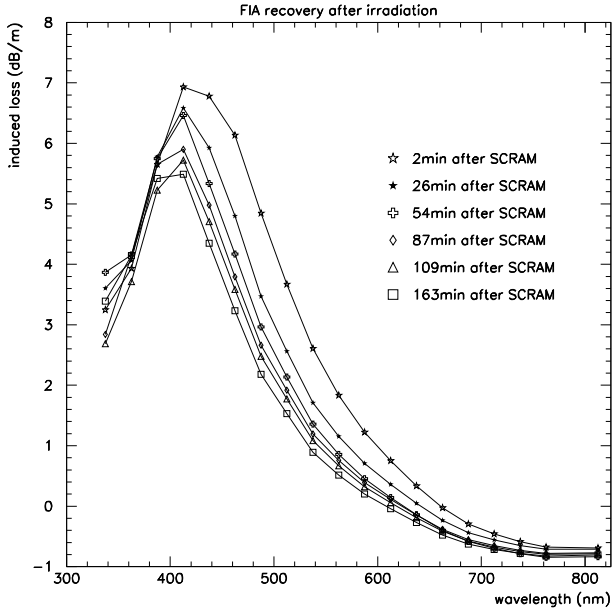

Figure 10: The post-irradiation optical transmission recovery of the FIA-type fiber is shown above at six different times at the end of the third day of reactor operation. Note that there is a speedy recovery after 2 minutes and the recovery profile follows the damage profile back in time.

calorimeter performance should be addressed.

4. The fast neutron irradiation in a cyclotron seems to damage the silica-core fibers faster ($b \approx 0.49$) than the fission neutrons ($b \approx 0.25$) from a reactor (Table 2).

5. For the same IN-type fiber, < 10 MRad γ-irradidation seems to have generated a similar type of optical damage to as neutrons at a fluence of 10^{15} n/cm^2 [18]. More detailed comparisons between these data sets can be misleading since the experimental systematics may be quite different.

6. The intent with these initial neutron irradiation studies was to establish a general method of testing individual fibers which was specifically aimed at the needs of the forward calorimeter. We only reported some of the irradiation results from neutrons, but identical apparatus and analyses procedures were used at LIL at CERN with 0.5 GeV electrons. We will report on them in a future note. Our plans call for improved systematic errors and a methodical testing of different fibers from various suppliers in order to select the best fiber for the HF.

5 Acknowledgements

We thank Scott Wendt and Tom Zimmerman for running the ISU reactor; and Laszlo Buday, Imre Erdody, Lazslo Juhos, Zoltan Kormany, Pal Kovacs, Sandor Kulcsar and Endre Madarasz for operating the MGC-20E cyclotron at ATOMKI. Thanks also go to Gary Nelson of Polymicro Inc. for supplying some of the fiber samples. This work was supported in part by the U.S. Department of Energy, the Hungarian Research Fund (OTKA), Contract No. T026184 and the Scientific and Technical Research Council of Turkey, TUBITAK.

References

[1] *The Hadron Calorimeter Project, Technical Design Report*, CERN/LHCC 97-31, 20 June 1997.

[2] N. Akchurin *et al.*, Nucl. Inst. and Meth. A 399 (1997) 202

[3] K. Gill *et al.*, *Gamma and Neutron Radiation Damage Studies of Optical Fibers*, CERN-ECP/96-13, October 1996 also submitted to Journal of Non-crystalline Solids.

[4] The neutron spectrum for fission of U^{235} can be represented by a semiempirical equation, $n(E) \sim \exp(-E/0.965)\sinh(\sqrt{2.29E})$. See *Proceedings of the International Conference on the Peaceful Uses of Atomic Energy*, Vol.2 (New York: United Nations, 1956), p.193.

[5] A. Fenyvesi *et al.*, *Package irradiation studies*, CERN/DRDC/RD-16/FERMI Note-14, CERN, Geneva, Switzerland, (January 1993) and M. A. Lone *et al.*, NIM **143** (1977) 331-344.

[6] K. Nagasawa, Y. Hoshi, Y. Ohki and K. Yahagi, Jpn. J. Appl. Phys. **25**, 464 (1986) and K. Nagasawa, R. Tohmon, and Y. Ohki, Jpn. J. Appl. Phys. **26**, 148 (1987).

[7] D. L. Griscom and E. J. Friebele, Phys. Rev. B. **34**, 7524 (1986).

[8] H. Hanafusa, Y. Hibino and F. Yamamoto, J. Appl. Phys., **58**, 1356-1361 (1985).

[9] D. L. Griscom, *The Centennial Memorial Issue of The Ceramic Society of Japan*, 1991.

[10] D. Griscom, J. Appl. Phys. Vol 80, No. 4 (1996) 2142-2155

[11] E. Lell, N. J. Kreidl and J. R. Hensler, in *Progress in Ceramic Science*, edited by J. Burke, (Pergamon Press, Oxford, New York, 1966).

[12] H. Hayami *et al.*, *Improvement in Radiation Resistivity of Pure Silica Core Image Guides for Industrial Fiberscopes*, Mitsubishi Cable Industries, Ltd. preprint.

[13] A. Utsumi *et al.*, SPIE Vol. 506, Fiber Optics in Adverse Environments II 176-181 (1984).

[14] E. J. Friebele and M. E. Gingerich, App. Optics, **20** (1981) 3448-3452

[15] A. N. Gurzhiev *et al.*, *Radiation Hardness of Optical Fibers*, IHEP 95-121, Protvino 1995.

[16] J. K. Partin, SPIE Vol.506, Fiber Optics in Adverse Environments II (1984).

[17] A. Uzunian, private communication (CMS/HF tdr130 setup).

[18] V. Gavrilov *et al.*, CMS/TN 94-324.